Synthesis and structural characterization of $CoMn_2O_4$ binary metal oxide from metal-organic frameworks

Nguyen Van Bang*, Nguyen Thi Phuong

Institute of Materials, Biology and Environment, Academy of Military Science and Technology, 17 Hoang Sam, Nghia Do, Cau Giay, Ha Noi, Vietnam.
*Corresponding author: vbnguyenhh@gmail.com
Received 06 Mar. 2025; Revised 09 May 2025; Accepted 12 May 2025; Published 25 Jun. 2025.
DOI: https://doi.org/10.54939/1859-1043.j.mst.104.2025.79-86

ABSTRACT

The $CoMn_2O_4$ binary metal oxide with a spinel structure was synthesized from metal-organic framework (MOF) prepared using both microwave-assisted and hydrothermal methods. The time to synthesize MOF by hydrothermal method is much longer than that of the microwave-assisted method. Synthesized materials were characterized by X-ray diffraction (XRD), Fourier-transform infrared spectroscopy (FT-IR), scanning electron microscopy (SEM), and Brunauer-Emmett-Teller (BET) surface area. The results showed that the $CoMn_2O_4$ oxide had high purity and a spherical nanocrystalline morphology with particle sizes ranging from 30 nm to 50 nm. Notably, the specific surface area of the material derived from MOF synthesized using the microwave-assisted method reaches 92,40 m^2/g, significantly higher than that of the material synthesized by the hydrothermal method, which is 61,84 m^2/g This demonstrates that the microwave-assisted method not only reduces synthesis time but also enhances the specific surface area of the material, which is a crucial factor for applications in catalysis, energy storage, and environmental treatment.

Keywords: $CoMn_2O_4$; Metal-organic framework; XRD; EDX; FTIR; SEM; BET.

1. INTRODUCTION

In response to the increasing energy demands and environmental challenges, research on advanced materials for energy storage and pollution treatment has become increasingly important. Advances in materials science contribute to improving sustainable energy systems and reducing environmental impacts. Notably, transition metal oxides with superior electrochemical properties and efficient charge transport have emerged as potential candidates for energy conversion and environmental remediation.

Spinel-structured metal oxides, represented by the general formula AB_2O_4, have attracted significant research interest in energy storage [1], photocatalysis [2], sensing [3], and optoelectronics [4]. Due to their controllable composition, valence states, and structure, they exhibit outstanding catalytic properties [5] and hold great potential as electrode materials for lithium-ion batteries and supercapacitors. Recently, MOF-derived $CoMn_2O_4$ has been investigated as an electrode material due to its large surface area, excellent electrochemical properties, and high stability [6]. The heterojunction between two metal oxides enhances charge separation, improving photocatalytic activity [7, 8], while also increasing electrical conductivity and providing more active sites, thus boosting supercapacitor performance [9]. Cobalt-based heterogeneous catalysts exhibit high catalytic activity and a slow Co^{2+} release rate [10, 11]. The combination of cobalt oxide with manganese - an abundant, low-toxicity element with multiple valence states favorable for redox reactions - has been explored in previous studies [12, 13].

Spinel compounds can be synthesized using various methods such as the sol-gel method [14, 15], coprecipitation method [16, 17], solvothermal method [18],… However, these methods have limitations, including difficulties in precisely controlling the composition, morphology, and porosity of the synthesized oxides. Metal-organic frameworks, which consist of metal centers coordinated

with organic molecules to form one-, two-, or three-dimensional porous structures, have emerged as promising templates for synthesizing transition metal oxides with tunable chemical composition, morphology, and porosity [19]. MOFs exhibit outstanding properties, including a large surface area and adjustable pore sizes, making them highly versatile for various applications such as sensing [20], supercapacitors [21], photocatalysis [22], and gas separation [23].

In this study, the research team synthesized the binary metal oxide $CoMn_2O_4$ using MOF-derived materials prepared by two different methods: microwave-assisted and hydrothermal synthesis.

2. EXPERIMENT AND METHOD

2.1. Chemicals, equipment and instruments

2.1.1. Chemicals

$Co(NO_3)_2 \cdot 6H_2O$ 99% (Xilong, China); $MnCl_2 \cdot 4H_2O$ 99% (Xilong, China); 1,3,5-Benzenetricarboxylic acid 98% (H_3BTC) (Macklin, China); Ethanol 99.7% (Xilong, China); N,N-Dimethylformamide 99.5% (Xilong, China); distilled water.

2.1.2. Equipment and instruments

Glassware set (beakers, glass rods, graduated cylinders, glass funnels, etc.), magnetic stirrer with heating (HPS-20, Fcombio-USA, China), drying oven (DHG-9145A, Bluepard, China), analytical balance (PA 213, Ohaus-USA, China), hydrothermal autoclave, Duran glass bottle (Germany), high-temperature furnace (Nabertherm GmbH, Germany), microwave oven (Electrolux EMM2022MW, China), ultrasonic cleaner (JP-060S, Skymen, China), high-speed centrifuge (Hettich, Universal 320, Germany).

2.2. Synthesis of binary metal oxide $CoMn_2O_4$ based on metal-organic framework $CoMn_2$-BTC

The synthesis of $CoMn_2$-BTC via the microwave-assisted method was carried out by dissolving 0,02 mol $Co(NO_3)_2 \cdot 6H_2O$ and 0,04 mol $MnCl_2 \cdot 4H_2O$ in 210 mL of solvent mixture (distilled water, N,N-dimethylformamide, and ethanol in a 1:1:1 volume ratio). Then, 0.1 mol of 1,3,5-Benzenetricarboxylic acid was added, and the solution was ultrasonicated for 30 minutes to achieve homogeneity. The resulting mixture was transferred into a Duran glass bottle, placed in a microwave oven, and maintained at 200 W power for 60 minutes with a cycle of 5 minutes of irradiation followed by 1 minute of rest. This cycle was selected based on preliminary optimization to avoid overheating, stabilize the temperature, enhance diffusion, and promote more uniform MOF crystal growth. The obtained MOF $CoMn_2$-BTC was washed multiple times with ethanol and dried at 80 °C for 5 hours.

For the hydrothermal method, the initial procedure was similar to the microwave-assisted method. However, after homogenization, the solution was transferred into a Teflon-lined autoclave and maintained at 150 °C for 24 hours. The resulting solid precipitate was filtered, washed, and dried at 80 °C for 5 hours.

Finally, the synthesized MOF was calcined at 400 °C for 4 hours in air with a heating rate of 10 °C/min, then cooled to room temperature to obtain the black binary metal oxide $CoMn_2O_4$.

2.3. Methods for material characterization

Phase composition was analyzed using X-ray diffraction (XRD), morphology was examined using scanning electron microscopy (SEM) and the chemical composition was analyzed by Energy Dispersive X-ray Spectroscopy (EDX) at the Institute of Materials Science (Vietnam Academy of Science and Technology).

Chemical bonding groups and material formation were determined through Fourier-transform infrared spectroscopy (FT-IR) and Surface parameters were measured by the nitrogen adsorption isotherm method (BET analysis) at the Institute of Chemistry and Materials (Academy of Military Science and Technology).

3. RESULTS AND DISCUSSION

X-ray diffraction (XRD) analysis was used to determine the phase purity and crystal structure of the MOF $CoMn_2$-BTC and $CoMn_2O_4$ materials, and the XRD patterns are shown in figure 1a.

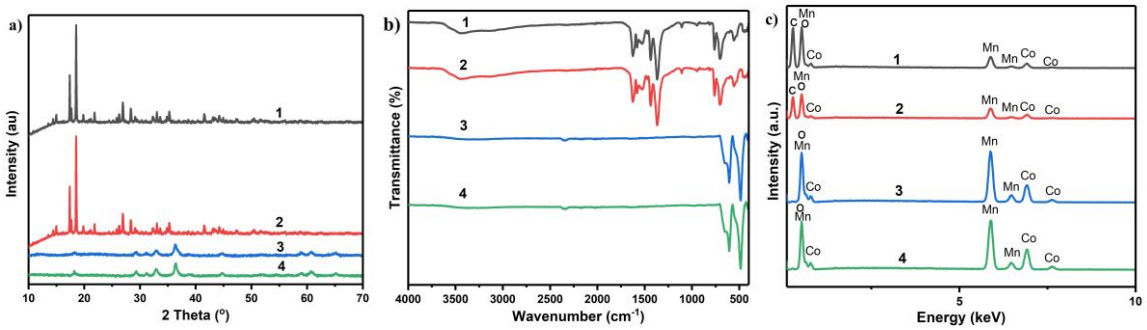

Figure 1. *XRD patterns (a), FTIR spectra (b), and EDX spectra (c) of the $CoMn_2$-BTC (1, 2) and $CoMn_2O_4$ (3, 4) materials: 1, 3 - synthesized by the microwave-assisted method; 2, 4 - synthesized by the hydrothermal method.*

The XRD pattern of the MOF $CoMn_2$-BTC material (figure 1a), synthesized by both methods, exhibits sharp diffraction peaks at 2θ values of approximately 14,99°, 17,39°, 17,69°, 18,55°, 19,83°, 21,85°, 26,92°, 28,35°, 33,04°, 35,27°, and 41,57°, consistent with previously reported data [24]. The crystal structure of this compound belongs to the monoclinic space group. The XRD patterns of $CoMn_2O_4$ derived from MOF (figure 1a), synthesized using both methods, completely match the standard JCPDS card No. 77-0471, confirming the successful synthesis of $CoMn_2O_4$ [18]. Additionally, no other peaks were observed in the XRD spectra, indicating the high phase purity of the synthesized material. The sharp and narrow peaks demonstrate that the obtained material possesses good crystallinity. The XRD patterns of materials synthesized by both methods exhibit distinct diffraction peaks at 2θ angles ~ 18,28°, 29,33°, 31,11°, 32,92°, 36,31°, 38,67°, 44,74°, 50,50°, 51,78°, 54,33°, 56,53°, 59,44°, 60,63°, and 65,17°, corresponding to the (101), (112), (200), (103), (211), (202), (220), (204), (105), (312), (303), (321), (224), and (400) crystal planes of $CoMn_2O_4$. The crystal structure of this oxide exhibits distortions and crystallizes in the tetragonal system with the $I4_1/amd$ space group. This phenomenon is commonly attributed to the Jahn-Teller effect of Mn^{3+} ions, which induces crystal lattice distortions [18].

Figure 1b presents the FTIR spectrum of the $CoMn_2$-BTC and $CoMn_2O_4$ materials in the wavelength range of 4000 cm^{-1} to 400 cm^{-1}. For the $CoMn_2$-BTC sample (figure 1b), IR absorption bands observed in the range of 3100 - 3600 cm^{-1} are attributed to the stretching vibrations of O–H bonds. Additionally, bands in the ranges of 1367 - 1437 cm^{-1} and 1530 - 1630 cm^{-1} correspond to the symmetric and asymmetric stretching vibrations of the $–COO^–$ groups, respectively. In-plane stretching vibrations of C–C bonds were detected around 1108 cm^{-1}. The bands at ~703 cm^{-1} and 762 cm^{-1} are associated with in-plane and out-of-plane bending vibrations of C–H in the benzene ring.. The FTIR spectrum of the $CoMn_2O_4$ material (figure 1b) shows distinct absorption bands in the low-wavenumber region (800 - 400 cm^{-1}). The absorption peaks at 606,66 cm^{-1} and 485,20 cm^{-1} are attributed to the stretching vibrations of Mn–O and Co–O bonds, respectively. Apart from these characteristic absorption bands, no additional peaks were observed, indicating the high purity of the synthesized product, free from impurities. This result is entirely consistent with the X-ray diffraction (XRD) analysis, further confirming the homogeneity and high quality of the obtained material.

The chemical composition of the MOF and oxide materials was analyzed by EDX, with results shown in table 1 and figure 1c.

Table 1. *Elemental composition of the $CoMn_2$-BTC and $CoMn_2O_4$ oxide materials.*

Element	Microwave-assisted method				Hydrothermal method			
	$CoMn_2$-BTC		$CoMn_2O_4$		$CoMn_2$-BTC		$CoMn_2O_4$	
	Weight, %	Atomic, %	Weight, %	Atomic, %	Weight, %	Atomic, %	Weight, %	Atomic, %
C K	40.21	51.32	-	-	37.49	50.16	-	-
O K	47.25	45.27	30.53	60.73	44.49	44.69	29.23	59.30
Mn K	8.04	2.24	44.98	26.05	11.82	3.46	43.04	25.43
Co K	4.51	1.17	24.49	13.22	6.20	1.69	27.73	15.27
Tổng	100							

The EDX analysis results reveal a clear difference in chemical composition between the MOF samples and the oxides formed after calcination. In the MOF samples synthesized by both the microwave-assisted and hydrothermal methods, the main elements detected were C, O, Mn, and Co. After calcination of the MOF samples to form oxides, carbon was completely eliminated from the structure, confirming the complete decomposition of the BTC organic framework. Simultaneously, the contents of Mn and Co significantly increased, reaching approximately 44 - 45% and 24 - 28% by weight, respectively. The atomic Co:Mn ratios in both oxide samples were approximately 0,5 - 0,6, which is close to the theoretical ratio of the spinel $CoMn_2O_4$ phase (Co:Mn = 1:2), suggesting that the obtained oxides are likely bimetallic oxides with a spinel structure. This result is also consistent with the XRD analysis discussed above.

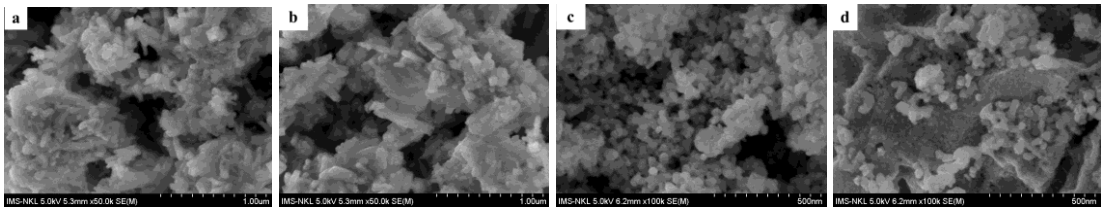

Figure 2. *SEM images of $CoMn_2$-BTC (a, b) and $CoMn_2O_4$ (c, d): a, c - Synthesized by the microwave-assisted method; b, d - Synthesized by the hydrothermal method.*

To analyze the morphology of the synthesized products, scanning electron microscopy (SEM) was employed. The SEM images of the $CoMn_2$-BTC and the bimetallic oxide $CoMn_2O_4$ materials are presented in figure 2. From the SEM images, it can be observed that the $CoMn_2$-BTC crystals synthesized by both methods exhibit a rod-like morphology. The crystal sizes are relatively uniform, with widths ranging from 80 -100 nm and lengths between 200 - 220 nm. In contrast, the $CoMn_2O_4$ materials synthesized from the MOF precursors by both methods show spherical nanocrystalline morphology, with particle sizes ranging from 30 nm to 50 nm. Using the Scherrer equation, $D = K \cdot \lambda / (\beta \cdot \cos\theta)$ (where D = crystallite size (nm), K = 0,9 (Scherrer constant), λ = 0,15406 nm (X-ray wavelength), β = FWHM (radians) and θ = peak position (radians)), the average crystallite sizes were calculated at the highest-intensity peaks: 18,552° for MOF and 36,31° for $CoMn_2O_4$. The results were approximately 91 nm and 24 nm, respectively. The particle size distribution was relatively uniform for both synthesis methods, indicating that both approaches offer effective control over particle morphology and size. However, the $CoMn_2O_4$ nanoparticles tend to aggregate, likely due to Van der Waals forces and electrostatic interactions between particle surfaces. Additionally, the aggregation may stem from the initial MOF precursors also exhibiting some degree of agglomeration (figures 2a and 2b). This aggregation may affect the active surface area of the materials and could require further treatment to improve particle dispersion, thereby optimizing performance in applications such as

catalysis or energy storage.

The N_2 adsorption-desorption isotherm, pore size and volume distribution curves of the $CoMn_2$-BTC and $CoMn_2O_4$ material are shown in figure 3 and figure 4, respectively. The measurement parameters for the MOF and oxide materials synthesized by both the hydrothermal and microwave-assisted methods are summarized in table 2.

From figure 3, it can be observed that the nitrogen adsorption-desorption isotherms of the $CoMn_2$-BTC and $CoMn_2O_4$ materials synthesized by both methods correspond to type IV isotherms with H3 hysteresis loops, according to the IUPAC classification, indicating the presence of mesopores. This observation is further supported by the pore size and volume distribution curves, calculated using the BJH method, as depicted in figure 4. These mesopores are likely formed due to the aggregation and loosely packed arrangement of $CoMn_2O_4$ nanoparticles, as observed in the SEM images (figure 2).

Table 2. *Textural parameters obtained from N_2 desorption isotherm measurements of $CoMn_2$-BTC and $CoMn_2O_4$ materials.*

Parameter	**Microwave-assisted method**		**Hydrothermal method**	
	$CoMn_2$-BTC	**$CoMn_2O_4$**	**$CoMn_2$-BTC**	**$CoMn_2O_4$**
Specific surface area (BET), m^2/g	100,25	92,40	77,65	61,84
Pore diameter, nm	3,77	3,23	3,38	3,41
Pore volume, cm^3/g	0,089	0.435	0,085	0.228

The specific surface area of $CoMn_2O_4$ was calculated using the BET method. The results presented in table 1 indicate that the MOF-derived $CoMn_2O_4$ synthesized via the microwave-assisted and hydrothermal methods yielded materials with specific surface areas of 92,40 m^2/g and 61,84 m^2/g, respectively. Specific surface area is a crucial parameter for porous materials, influencing their potential applications. $CoMn_2O_4$ with a high specific surface area enhances ion storage and diffusion capabilities, making it suitable for battery and supercapacitor fabrication, improving charge storage performance. Additionally, a larger surface area increases adsorption capacity and provides more active sites for surface reactions, making it valuable as a catalytic material. The $CoMn_2O_4$ synthesized by our research group exhibits a significantly higher BET surface area compared to some previous reports: sol-gel method (31 m^2/g [14], 24,23 m^2/g [15]), solvothermal method (36 m^2/g [18]), and coprecipitation method (14 m^2/g [14]). The $CoMn_2O_4$ synthesized from metal-organic frameworks retains the highly porous nature of the precursor MOF. Upon conversion to metal oxide, the porous structure is preserved, maintaining a large surface area for the oxide material.

Both synthesis methods employed in this study yielded oxides with high specific surface areas. However, the specific surface area of $CoMn_2O_4$ derived from MOF synthesized via the microwave-assisted method was significantly higher at 92,40 m^2/g compared to 61,84 m^2/g for the hydrothermal method. This result also surpasses some previously reported $CoMn_2O_4$ oxides synthesized from MOF precursors: 31,43 m^2/g for MOF synthesized via the hydrothermal method [25] and 63,3 m^2/g for MOF synthesized via mechanochemical methods [26]. The difference in surface area may be attributed to the fact that the MOF precursor synthesized using the microwave-assisted method resulted in a MOF with a higher specific surface area than that obtained through the hydrothermal method. The microwave-assisted approach enables rapid and uniform heating, reducing reaction time. This process minimizes particle agglomeration and growth, producing smaller, more uniformly distributed particles with well-developed porous structures, leading to a higher specific surface area. In contrast, the hydrothermal method involves slow heating in a sealed high-pressure environment with prolonged reaction times. This

can lead to particle aggregation and the formation of larger particles, ultimately reducing the specific surface area.

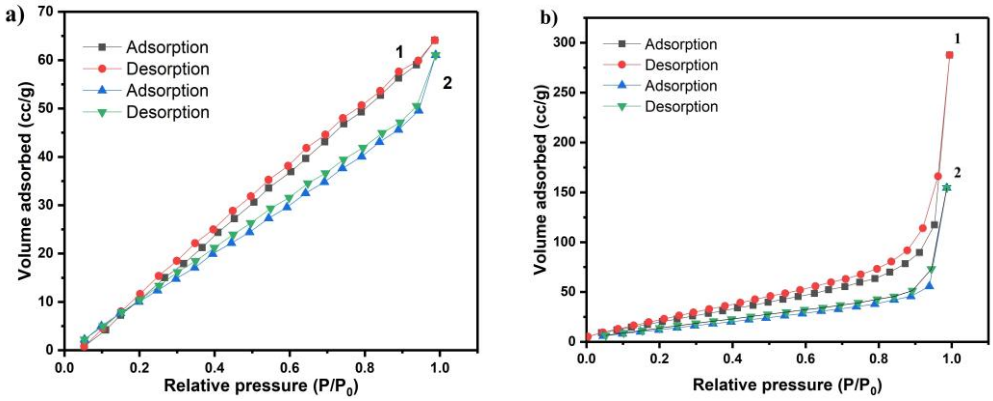

Figure 3. *The nitrogen adsorption-desorption isotherms of $CoMn_2$-BTC (a) and $CoMn_2O_4$ (b): 1 - Synthesized by the microwave-assisted method; 2 - Synthesized by the hydrothermal method.*

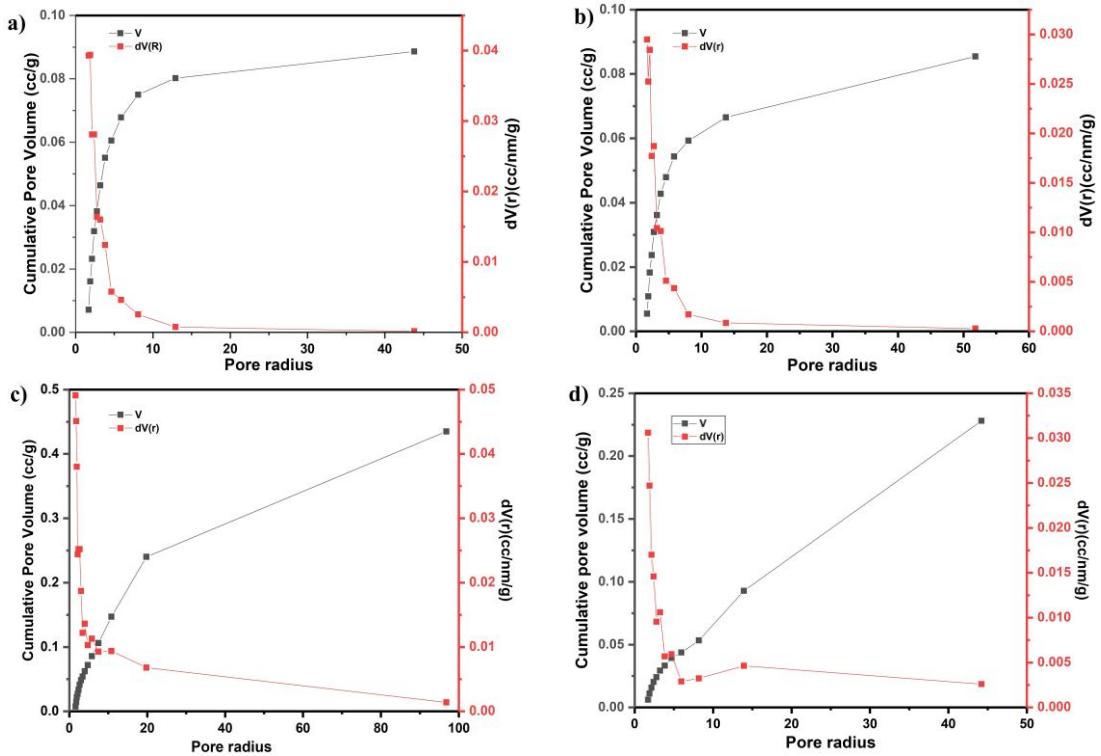

Figure 4. *Pore size and volume distribution curve of MOF (a, b) and $CoMn_2O_4$ (c, d): a, c - Synthesized by the microwave-assisted method; b, d - Synthesized by the hydrothermal method.*

Thus, the research team successfully synthesized $CoMn_2O_4$ based on MOF using the microwave-assisted method, achieving a significantly shorter reaction time (60 minutes) compared to the conventional hydrothermal method (24 hours). Reducing the synthesis time not only improves process efficiency but also lowers energy consumption, contributing to cost optimization. Additionally, this method minimizes solvent usage and reduces waste generation, aligning with the principles of green chemistry - an important trend in the development of advanced and sustainable materials.

4. CONCLUSIONS

The research team successfully synthesized the bimetallic oxide $CoMn_2O_4$ based on metal-organic framework materials using two different methods: microwave-assisted and hydrothermal synthesis. Both methods produced high-purity materials with no detectable impurities, demonstrating the efficiency of the synthesis process. Notably, the obtained materials exhibited a larger specific surface area (BET) compared to some previous reports. Between the two methods, the specific surface area of $CoMn_2O_4$ derived from MOF synthesized via the microwave-assisted method reached 92,40 m^2/g, significantly higher than 61,84 m^2/g obtained through the hydrothermal method. This highlights the advantage of the microwave-assisted approach in controlling the material's microstructure. Moreover, the microwave-assisted method offers a significantly shorter synthesis time compared to the hydrothermal method, leading to energy savings, reduced risks during fabrication, and ease of implementation with simple equipment. This not only enhances manufacturing efficiency but also aligns with the trend of green chemistry, promoting the development of sustainable and environmentally friendly materials.

Acknowledgement: *This study was conducted with financial support from the 2025 Ministry of Industry and Trade-level science and technology project.*

REFERENCES

[1]. Gonçalves J. M. et al., *" Multifunctional spinel $MnCo_2O_4$ based materials for energy storage and conversion: A review on emerging trends, recent developments and future perspectives*", Journal of Materials Chemistry A, 9 (6), (2020).

[2]. Suresh R. et al., "*Recent advancements of spinel ferrite based binary nanocomposite photocatalysts in wastewater treatment*", Chemosphere, 274, 129734, (2021).

[3]. Gonçalves J. M. et al., *"Feasible strategies to promote the sensing performances of spinel Mco_2O_4 (M = Ni, Fe, Mn, Cu and Zn) based electrochemical sensors: a review",* Journal of Materials Chemistry C., 9, pp. 7852 - 7887, (2021).

[4]. Yadav et al., *"Polypropylene Nanocomposite Filled with Spinel Ferrite $NiFe_2O_4$ Nanoparticles and In-Situ Thermally-Reduced Graphene Oxide for Electromagnetic Interference Shielding Application",* Nanomaterials, 9(4), 621, (2019).

[5]. Q. Zhao et al., "*Spinels: Controlled Preparation, Oxygen Reduction/Evolution Reaction Application, and Beyond*", Chem. Rev., 117, pp. 10121 - 10211, (2017).

[6]. J. Zhao et al., "*Spinel $ZnMn_2O_4$ nanoplate assemblies fabricated via "escape-by-crafty-scheme" strategy*", Journal of Materials Chemistry, 22, pp. 13328-13333, (2012).

[7]. Suresh R. et al., "*Recent advancements of spinel ferrite based binary nanocomposite photocatalysts in wastewater treatment*", Chemosphere, 274, 129734, (2021).

[8]. Lai Y.J. et al., *"Solid mediator Z-scheme heterojunction photocatalysis for pollutant oxidation in water: Principles and synthesis perspectives"*, Journal of the Taiwan Institute of Chemical Engineers, 125, pp. 88 - 114, (2021).

[9]. Saha S. et al., "*A review on the heterostructure nanomaterials for supercapacitor application*", Journal of Energy Storage, 17, pp. 181 - 202, (2018).

[10]. T. Zeng et al., "*Spatial Confinement of a Co_3O_4 Catalyst in Hollow Metal-Organic Frameworks as a Nanoreactor for Improved Degradation of Organic Pollutants*", Environmental Science & Technology, 49, pp. 2350 - 2357, (2015).

[11]. P. Hu et al., "*Cobalt-catalyzed sulfate radical-based advanced oxidation: A review on heterogeneous catalysts and applications*", Applied Catalysis B-Environmental, 181, pp. 103 - 117, (2016).

[12]. H. Liang et al., "*Excellent performance of mesoporous Co_3O_4/MnO_2 nanoparticles in heterogeneous activation of peroxymonosulfate for phenol degradation in aqueous solutions*", Applied Catalysis B-Environmental, 127, pp. 330-335, (2012).

[13]. Y. Yao et al., "*Sulfate radicals induced from peroxymonosulfate by cobalt manganese oxides ($Co_xMn_{3-x}O_4$) for Fenton-Like reaction in water*". Journal of Hazardous Materials, 296, pp. 128-137, (2015).

[14]. Hosseini S. A. et al., "*Chemical-physical properties of spinel $CoMn_2O_4$ nano-powders and catalytic activity in the 2-propanol and toluene combustion: Effect of the preparation method*", Journal of Environmental Science and Health, Part A, 46(3), pp. 291 - 297, (2011).
[15]. Lin C. et al., "*$CoMn_2O_4$ Catalyst Prepared Using the Sol-Gel Method for the Activation of Peroxymonosulfate and Degradation of UV Filter 2-Phenylbenzimidazole-5-sulfonic Acid (PBSA)*", Nanomaterials, 9(5), 774, (2019).
[16]. Abel M. J. et al., "*Investigation on structural, optical and photocatalytic activity of $CoMn_2O_4$ nanoparticles prepared via simple co-precipitation method"*, Physica B Condensed Matter, 601(4), 412349, (2020).
[17]. John Abel M. et al., *"Facile synthesis of solar light active spinel nickel manganite ($NiMn_2O_4$) by co-precipitation route for photocatalytic application"*, Research on Chemical Intermediates, 46 (27), (2020).
[18]. Li Y. et al., "*Novel hollow microspheres $Mn_xCo_{3-x}O_4$ (x = 1, 2) with remarkable performance for low-temperature selective catalytic reduction of NO with NH_3"*, Journal of Sol-Gel Science and Technology, 81(2), pp. 576 - 585, (2016).
[19]. Masoomi M. Y. et al., *"Mixed-Metal MOFs: Unique Opportunities in Metal–Organic Framework (MOF) Functionality and Design"*, Angewandte Chemie, 131(43), pp. 15330 - 15347, (2019).
[20]. Hessamaddin Sohrabi et al., *"Metal-organic frameworks (MOF)-based sensors for detection of toxic gases: A review of current status and future prospects"*, Materials Chemistry and Physics, 299, 127512, (2023).
[21]. Yuxia Xu et al., *"Metal organic frameworks and their composites for supercapacitor application",* Journal of Energy Storage, 56 (A), 105819, (2022).
[22]. Qian Su et al., *"Research progress of MOF-based materials in the photocatalytic CO_2 reduction",* Carbon Resources Conversion, 7 (1), 100211, (2024).
[23]. Lin R. B. et al., *"Microporous Metal-Organic Framework Materials for Gas Separation*", Chem, 6 (2), pp. 337 - 363, (2019).
[24]. Linyan Yang et al., "*Bimetal-Organic Framework-Derived CoMn@C Catalysts for Fischer-Tropsch Synthesis*", Catalysts, 13(3), 633, (2023).
[25]. Li C. X. et al., *"Metal organic framework-derived $CoMn_2O_4$ catalyst for heterogeneous activation of peroxymonosulfate and sulfanilamide degradation"*, Chemical Engineering Journal, 337, pp. 101 - 109, (2018).
[26]. Zhao J. et al., "*Gas-solid two-phase flow (GSF) mechanochemical synthesis of dual-metal–organic frameworks and research on electrochemical properties*", Nanoscale Advances, 2(12), pp. 5682 - 5687, (2020).

TÓM TẮT

Nghiên cứu tổng hợp và đánh giá đặc trưng cấu trúc của vật liệu oxit hai kim loại $CoMn_2O_4$ trên cơ sở vật liệu khung kim loại-hữu cơ

Vật liệu oxit hai kim loại $CoMn_2O_4$ có cấu trúc spinel được chế tạo trên cơ sở vật liệu khung kim loại-hữu cơ (MOF) tổng hợp bằng phương pháp hỗ trợ vi sóng và phương pháp thuỷ nhiệt. Thời gian tổng hợp vật liệu khung kim loại-hữu cơ bằng phương pháp thủy nhiệt dài hơn nhiều so với phương pháp vi sóng. Vật liệu tổng hợp được đặc trưng bằng nhiễu xạ tia X (XRD), phổ hồng ngoại (FTIR), kính hiển vi điện tử quét (SEM) và diện tích bề mặt Brunauer-Emmett-Teller (BET). Kết qủa cho thấy oxit $CoMn_2O_4$ có độ tinh khiết cao, hình thái là các tinh thể hình cầu có kích thước nano với đường kích hạt trong khoảng từ 50 nm đến 60 nm. Đáng chú ý, diện tích bề mặt riêng của vật liệu thu được trên cơ sở MOF được tổng hợp bằng phương pháp hỗ trợ vi sóng đạt 92,404 m^2/g, cao hơn đáng kể so với vật liệu tổng hợp bằng phương pháp thủy nhiệt 61,841 m^2/g. Điều này cho thấy phương pháp hỗ trợ vi sóng không chỉ giúp giảm thời gian tổng hợp mà còn cải thiện diện tích bề mặt riêng của vật liệu, yếu tố quan trọng đối với các ứng dụng trong xúc tác, lưu trữ năng lượng và xử lý môi trường.

Từ khoá: $CoMn_2O_4$; Vật liệu khung kim loại-hữu cơ; XRD; EDX; FTIR; SEM; BET.